International Journal of Scientific Research in Science and Technology
Print ISSN: 2395-6011 | Online ISSN: 2395-602X (www.ijsrst.com)
© 2021 | IJSRST | Volume 8 - Issue 1

Different Dielectric properties of Synthesized Mesoporous Molecular Sieves Rice Husk Ash -SBA-16

Shete S.B.
Department of Electronics S.G.B. College, Purna, Maharashtra, India

ABSTRACT
Rice Husk is the by-product produce during rice milling. Sustainable use of Rice Husk Ash (RHA) and Rice Husk (RH) in Industrial Sector and other fields depends upon its physical and chemical properties. This research contributes holistic approach to the potential use of rice husk towards synthesis of meso-porous material than the traditional uses of husks. It not only reduces the cost of material but also results in the reduction of the environmental greenhouse effects. Attempts have been made to investigate crystallization kinetics of SBA -16. The various synthesis parameters were investigated during crystallization of SBA -16. The activation energy of crystallization kinetics of SBA -16 was calculated using Arrhenius equation and found to be 184.62 kJ / mole in the present system of synthesis.

Keywords. Rice Husk Ash, Pluronic F127, Crystallization Kinetics, Dielectric properties.

I. INTRODUCTION
Hazardous wastes are generated annually throughout the world by all industries and their disposal poses major challenges and serious environmental problems. This creates serious health risks, taking into account that the amount of discharged material is expected to increase in the future. In the recent years, there has been a growing interest to find creative ways not only to reduce natural waste and industrial hazard to overcome environmental pollution but also its effective utilization1.

As we know that, Rice is a primary source of food. Its production covers almost 1% of the Earth's surface. Globally, approximately 700 million tons of rice2 is produced every year. India is a major rice producing country and annul production of rice husk is approximately 20 million tons3. For every 100 kg of paddy milled, about 22% of husk is produced2.Even though some of this husk is converted into end product such as feedstock and adsorbent but most is either dumped as a waste or burnt openly, causing environmental and health problems. Therefore, one of the chief principles of green technology is to utilize the RHA as a raw material or renewable resource for making high value added, versatile materials rather than depleting, as it has high silica content (>90%).

Quite a lot of research groups have taken the advantage of this silica composition and made endeavors in making micro4 and mesoporous5 zeolitic materials synthesized from extracted silica through them. These materials have wide applications as adsorbents, in ion exchange, as molecular sieves, catalysts16-18 etc. Compared to conventional microporous zeolites, mesoporous materials possess many advantages such as high surface area, large pore size and an ordered structure6, 7.

Santa Barbra University discovered new family (SBA-n) of mesoporous materials, among them SBA -16 possesses hexagonal molecular sieves having fairly uniform pores with pore diameter of 20-100Å. They possesses large surface area (more than 900 m2/g), which is attractive for designing new selective heterogeneous catalyst in production of fine chemicals on large scale.

Our research endeavors the use of no-cost raw materials such as agro waste rice husk for our further investigations because it add value; reduce the cost and create effective utilization to protect the environment19-21. It has potential application in synthesis of highly useful porous materials used in water purification technology, as industrial catalyst, supporting materials, exchanger, molecular sieves etc.

II. METHODS AND MATERIAL

Experimental: Materials and Methods for Synthesis of mesoporous SBA -16:

Hydrothermal synthesis of SBA -16 was carried out in hydrothermal reactor at autogenous pressure under stirring conditions. The chemicals used during synthesis were Pluronic F127, Butanol, Hydrochloric acid, Deionized water etc.

The rice husk silica extraction was carried out using acid hydrolysis method. Initially the collected rice husk was washed with deionized water and then dried at 800C for 24h. This husk was then treated with 3.0 M HCl acid solution along with heating at 1000C. This hydrolyzed rice husk was rinsed with distilled water until pH reaches to 7, then it was again dried at 100°C for 24 h. Finally, the rice husk was calcined at 8000C for 4h in muffle furnace. The rice husk ash was mixed with 3.75 M NaOH solution and stirred overnight to extract the silicate from the ash.

The synthesis of silica SBA-16 was made as following.

Solution of 2.5 g of Pluronic F127 (Sigma Aldrich) in a mixture of 120 g of distilled water, 5 g of concentrated HCl (37%) and 7.5 g of butanol was first prepared. After one hour stirring at 45 oC, 12 g of RHA 4.5g were added and the mixture stirred for further 24h.The ultrasonic treatment is given at 45 min. The step was followed by a hydrothermal treatment of 24 h at 100oC in Teflon coated stainless steel autoclave. Drying of the as synthesized sample was performed at room temperature overnight part of the dry sample was calcined under air flow by increasing the temperature 1.5oC per minute up to550oC and maintaining it at this temperature for 6 h sample hereafter named calc-SBA-16. by Fabio et al.,15 The samples were synthesized at 600C, 700C, 800C and 900C and are nominated as RHA-SBA-16 (60, 70, 80 and 90) respectively. After the crystallization, the solids were filtered, washed with deionized water and dried at 1000C for 2h. The products were finally calcined at 5500C for 4.5hrs in air and has been evaluated by X-ray diffraction, N2-sorption studies etc.

Characterization:

To elucidate the structural features8, morphology9, pore architecture10, thermal stability11, adsorptive12 and catalytic behavior13, surface area14 etc: the synthesized samples are characterized by techniques such as XRD, N2-sorption, FTIR, etc.

III. RESULTS AND DISCUSSION

XRD-studies:

% Crystallinity = Sum of the peak heights of unknown material × 100 Sum of peak heights of standard material

Fig.1 shows the XRD patterns of the samples calcined at 450, 500, 550, 600 and 650^{0}C designated as RHA-SBA-16 (450, 500, 550, 600 and 650) respectively. As shown in the Fig.1RHA-SBA-16 (450), the XRD pattern obtained for the sample calcined at calcinations temperature 450^{0}C, the only reflection at (110) plane is more intense, it suggests that the material does not possess the well defined hexagonal arrays even after the calcination.

The diffractograms gained for the samples as increase in their calcination temperature from 500 to 650^{0}C shows three weak peaks along with single most intense peak with (110) reflection at 2θ value 1.12^0. The d_{110}value is shifted to a higher value up to 600^{0}C Fig. 1 RHA-SBA-16 (500, 550, and 600).In the low 2-theta region of 1^0–10^0, the XRD pattern at 550^{0}C exhibits all prominent diffraction peaks which could be indexed as (110), (200) (210) and etc. reflections, respectively. This is characteristics of long range ordered hexagonal array of parallel silica tubes in RHA-SBA-16mesoporous phase. Therefore, the sample calcined at 550^{0}C can be treated as 100 % crystalline sample. As calcinations temperature in advance increased above 600^{0}C, a considerable decline in the intensity of (110) peak and d_{110} value shifted to the somewhat inferior value indicates condensation of the silanol groups in the pore walls. This can direct to the reorganization of silica walls of RHA-SBA-16 accordingly decreasing the crystallinity very immaterially.

Even though at 600^{0}C, the long range order of hexagonal array and textural morphology is still preserved. This resembles that synthesized sample of RHA-SBA-16 is thermally unwavering up to 600^{0}C as accounted.On the other hand, if the calcination temperature is increased up to 650^{0}C and above, the hexagonal phase transforms into the lamellar form which on additional calcination crumples the structure which is reflected as the absence of XRD peaks in RHA-SBA-16 (600) at and above 650^{0}C.

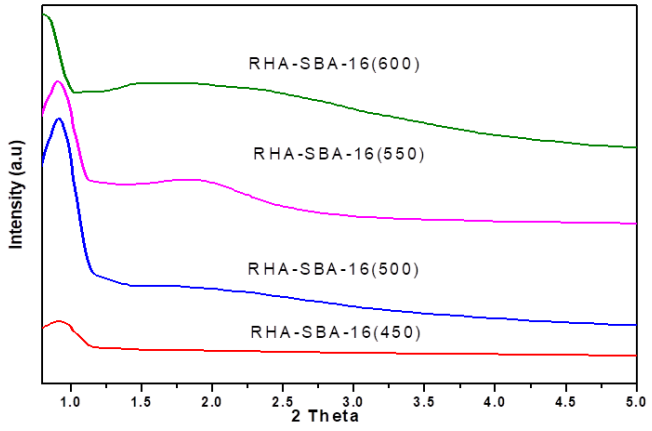

Fig. 1: (C) XRD patterns of calcined samples of RHA-SBA-16 (450, 500, 550, and 600) at various temperatures.

Therefore, the above results indicate that calcination temperature plays a noteworthy role to optimize the synthesis condition.

% Crystallinity and Activation Energy:

Table 1. Summarizes the values of inter planar spacing (d values) derived from X-ray diffraction pattern for RHA-SBA-16 (100% crystalline) sample. The percent crystallinity of the samples drawn at diverse calcination temperatures in the crystallization kinetics was calculated. The obtained values of % crystallinity were plotted as a function of calcination temperature from which the gradient of crystallization has been evaluated. The percent conversion from amorphous to100% crystalline product of RHA-SBA-16 phase is shown in the Fig. 2

Therefore, this most (100%) crystalline sample was used as a parent sample for further study.

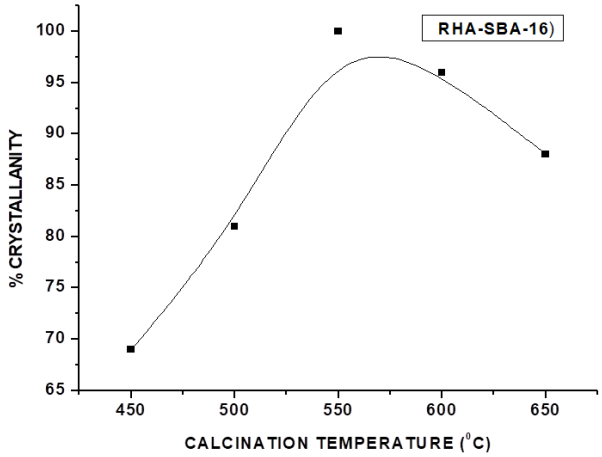

Fig.2 Effect of calcination temperature on crystallization

The kinetic curve describing the increase in the crystallinity of the crystals with the calcination temperature depends on rate of conversion. It is seen from the Fig.2 that upto 550^{0}C the rate of conversion of amorphous to crystallization of RHA-SBA-16 phase was very acute initially but followed by a subsequent slow down. Therefore, the rate of crystallization

decreases as the process approaches to the completion indicated by constancy (100 %) in percent crystallization.

Using Arrhenius equation to the kinetics of crystallization of RHA-SBA-16, activation energy was reported around 103.74kJ mole^{-1} in the present crystallization scheme.

BET surface area and pore volume of RHA-SBA-16:

The samples RHA-SBA-16 (450, 500, 550, 600 and 650) synthesized for 4.5h with different calcinations temperatures have also been characterized further by N2-sorption studies to find BET surface area and the corresponding pore size distribution. The adsorption-desorption curve obtained for RHA-SBA-16 (550, 600) is shown in the Fig3 These isotherms are of type IV as expected for SBA-16 molecular sieves.

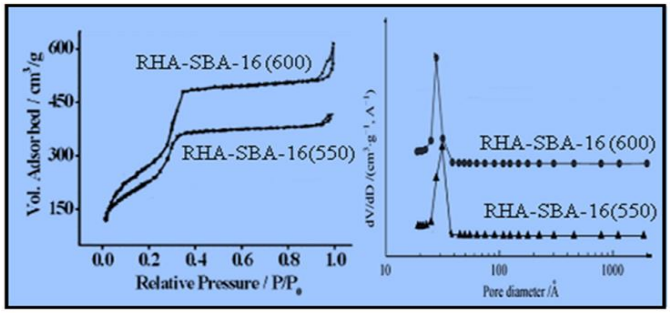

Fig .3 N2 adsorption-desorption isotherms and (B) pore size distribution of (a) RHA-SBA-16 (550^{0}C); (b) RHA-SBA-16 (600^{0}C)

The observations regarding N_2-sorption and XRD studies are statistically depicted in Table 1. From which we can conclude that, as the calcination temperature is increased after 550^{0}C, at the ramp of 1^{0}C, surface area got reduced by 1.5m^2/g. It is probably because of the collapse of gel structure due to the rapid release of water from the pores. Moreover, there is an auxiliary alteration in the average pore diameter and wall thickness. Pores with narrow distribution start forming from 500 ^{0}C and increases as calcination temperature increases. The mean wall thickness of the pores and pore volume increased with calcination temperature from 500^{0}C to 600^{0}C.

However, there is a slight decrease in wall thickness at the calcination temperature of 600^{0}C and above. These observations revels the hexagonal phase starts transforming to lamellar phase with lack of specific structural features, which are in well accordance with XRD patterns.

SEM and TEM-Analysis:

SEM images of RHA-SBA-16 (500, 600) are depicted in Fig.4 represents that the particles are nearly in spherical form exclusive of agglomerations. The typical diameter of the particles is moderately same although the calcination temperature is raised from 450^{0}C to 650^{0}C representing an excellent thermal stability. The diameter of spherical particles is found to vary in the range of 2.6A^0 to 9.98A^0, which is consistent with the XRD and N_2sorption data. The SEM photo graph of RHA-SBA-16 at 550^{0}C indicates a good structural morphology.

TEM-Analysis:

Fig.5 represents the TEM images of RHA-SBA-16synthesized at 80^{0}C and calcined at 550^{0}C. TEM image of the parent RHA-SBA-16samples provided sturdy verification of the retainment of mesoporous structure. The characteristic hexagonal silicate structures shown on TEM, supports the observation made by low angle XRD.

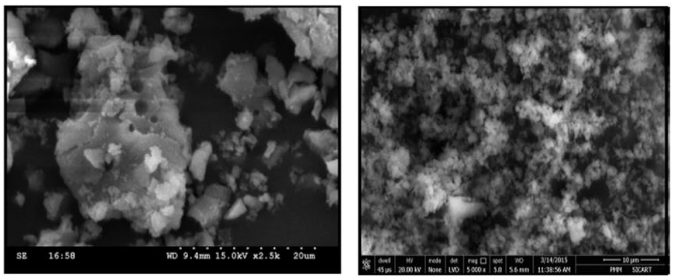

Fig. 4 SEM images of RHA-SBA-16 (500, 550) calcined at 500and 5500C

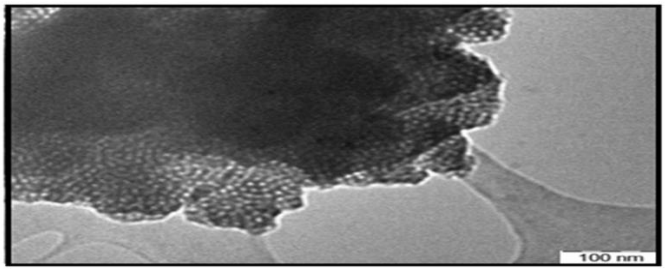

Fig. 5 TEM images of RHA-SBA-16 (550) calcined at 550^{0}C

Table 1 : Effect of calcination temperature on Structural and textural properties of RHA-SBA-16

Sample	d_{110}	Unit cell parameter	S.A. (m^2/g)	Average pore diameter (Å)	Pore volume (ml/g)	Average Wall thickness (Å)	% Crystal-linity
RHA-SBA-16(450)	22.15	31.90	–	–	–	–	69
RHA-SBA-16(500)	23.51	33.85	618.21	26.38	0.479	7.47	81
RHA-SBA-16(550)	26.93	38.78	779.70	29.16	0.568	9.62	100
RHA-SBA-16(600)	25.89	37.28	767.13	28.25	0.547	9.03	96
RHA-SBA-16(650)	24.21	34.86	738.22	26.99	0.506	7.87	88

Dielectric properties : The sample used for dielectric properties as RHA-SBA-16 (550) .For preparing the pallets Polly vinyl alcohol (PVA) is used as binder Pallets 10mm diameter were made and mass of pallet were measured also the thickness of pallet were measured .To remove the binder from the sample the pallets were kept in furnace at 200^{0}C for 2 hrs.The readings were taken on the reading impedance analyzer HIOKI model No.IM 3570

Fig.6 shows the frequency variation of dielectric constant for the samples of RHA-SBA-16. It can be observed from the figure that the dielectric constant for the samples decreases with increase in frequency.

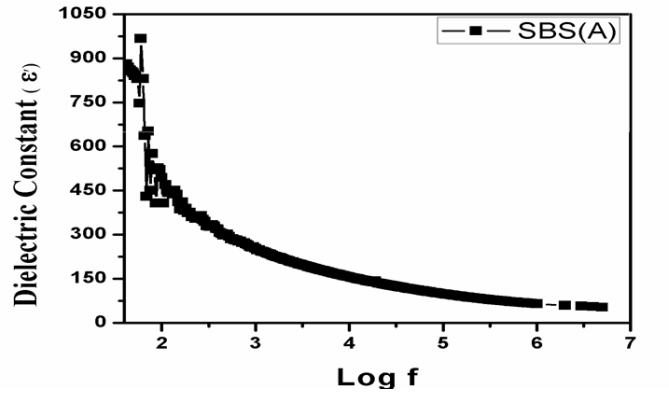

Fig.6 Dielectric constant and the frequency variation

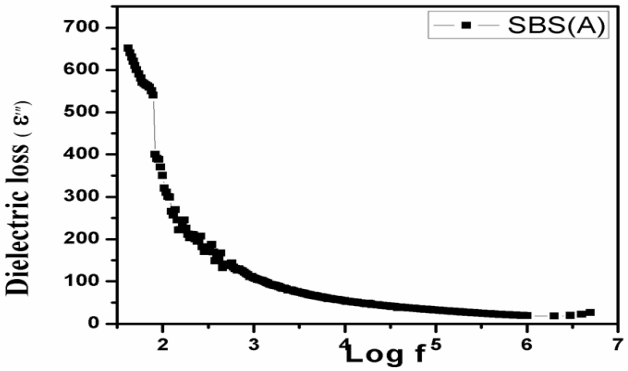

Fig.7 Dielectric loss with the frequency variation

Fig.7 shows the frequency variation of dielectric loss for the samples of RHA-SBA-16. It can be observed from the figure that the loss shows that the dissipation for the samples decreases with

Increase in frequency[22].

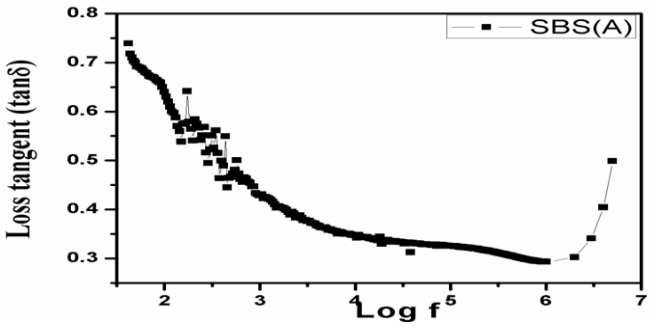

Fig.8 loss tangent with the frequency variation

Fig.8 shows the frequency variation of loss tangent for the samples of RHA-SBA-16. It can be observed from

the figure that the loss tangent for the samples decreases exponentially with Increase in frequency.

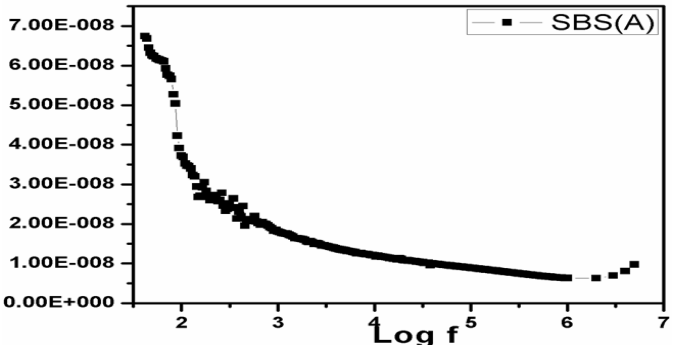

Fig.9ac conductivity with the frequency variation

Fig.9shows the frequency variation with ac conductivity for the samples of RHA-SBA-16. It can be observed from the figure that ac conductivity of the samples decreases exponentially with Increase in frequency.

IV. CONCLUSION

All the characterization techniques performed in this study reveals that well ordered mesoporous material of uniform hexagonal array can be synthesized very conveniently and in a very short span of time from an agro waste rice husk ash instead of commercial expensive silica sources. The parametric variation such as change of synthesis temperature helps to optimize the synthesis conditions. The well ordered mesoporous material RHA-SBA-16 can be synthesized at 80^0C for 4.5h keeping pH of gel 6.9 and calcined at 550^0C.The apparent activation energy of conversion of synthesis gel to 100 % crystalline RHA-SBA-16 phase was 184.62kJ/mole calculated by Arrhenius equation. The different dielectric characteristics are analyzed for the sample RHA-SBA-16.

V. REFERENCES

[1]. C.L. Carlson, D.C. Adriano, Environmental impact of coal combustion residue, J. Environ. Qual. 22, 227–247, (1993).

[2]. FAO Food Outlook, Food and Agriculture Organization of the United Nations, November, (2011).

[3]. www. maps of world.com.

[4]. Corma, A. Chem. Rev. 95, 559-614, (1995).

[5]. Kresge, C. T.; Leonowicz, M. E.; Roth, W. J.; Vartulli, J. C. U.S. Patent 5, 098, 684, (1992).

[6]. Schulz-Ekloff G, Stud. Surf. Sci. Catal., 85, p. 145, (1994).

[7]. Behrens P, Stucky G D, Angew. Chem. Intl. Ed. Engl., 32, p. 696, (1993).

[8]. J. R. Matos, M. Kruk, L. P. Mercuri, M. Jaroniec, T. Asefa, N. Coombs, G. A. Ozin, T. Kamiyama, and O. Terasaki, Chem. Mater. 14, 1903, (2002).

[9]. F. Kleitz, D. Liu, G. M. Anilkumar, I. S. Park, L. A. Solovyov, A. N. Shmakov, and R. Ryoo, J. Phys. Chem. B. 107, 14296 (2003).

[10]. J. Wloch, M. Rozwadowski, M. Lezanska, K. Erdmann, Analysis of the pore structure of the MCM-41 materials, Appl. Surf. Sci. 191, 368–374, (2002).

[11]. V. Parvulescu, S. Cman,V.I.Parvulescu,P.Grange,G.Poncelet, J. Catal. 180, 66, (1998).

[12]. Branton, P. J.; Hall, P. G.; Sing, K. S. W. J. Chem. Soc., Chem. Commun. 1257, (1993).

[13]. H. Van Bekkum, E.M. Flanigen, P.A. Jacobs, J.C. Jansen, Introduction to Zeolite Science and Practice, Elsevier, (2001).

[14]. Gregg, S. J.; Sing, K. S. W. Adsorption, Surface Area and Porosity, Second ed.; Academic Press INC. (London) LTD: London, (1982).

[15]. J.S. Beck, J.C. Vartuli, W.J. Roth, M.E. Leonowicz, C.T. Kresge, K.D. Schmitt, C.T.W Chu, D.H. Olson, E.W. Sheppard, S.B. McCullen, J.B. Higgins, J.L. Schlenker, J. Am. Chem. Soc. 114 (1992) 10834.

[16]. C.T. Kresge, M.E. Leonowicz, W.J. Roth, J.C. Vartuli, J.S. Beck, Nature 359 (1992)710.

[17]. C. Boissiere, M. Kummel, M. Persin, A. Larbot and E. Prouzet, Adv. Funct. Mater. 11 (2001) 129.

[18]. H.B.S. Chan, P.M. Budd, T.D. Naylor, J. Mater. Chem.11 (2001) 951.

[19]. Y. Sakamoto, M. Kaneda, O. Terasaki, D.Y. Zhao, J.M. Kim, G. Stucky, H.J. Shin, R. Ryoo, Nature 408 (2000) 449.

[20]. D. Zhao, Q. Huo, J. Feng, B.F. Chmelka, G.D. Stucky, J. Am. Chem. Soc. 120 (1998) 6024.

[21]. P. van der Voort, M. Benjelloun, E.F. Vansant, J. Phys. Chem. B 106 (2002) 9027.

[22]. Tatsuo Ohgushi and Kazushi Ishimaru, Phys. Chem.Chem.Phys., 3 (2001) 3229- 3234.